Selective hydrogenation of cinnamaldehyde in supercritical CO_2 over Me–CeO_2 (Me = Cu, Pt, Au): Insight of the role of Me–Ce interaction

C.M. Piqueras [a], V. Puccia [a], D.A. Vega [b], M.A. Volpe [a,*]

[a] Planta Piloto de Ingeniería Química, PLAPIQUI-Universidad Nacional del Sur-CONICET, Camino La Carrindanga km 7-CC 717, 8000 Bahía Blanca, Argentina
[b] Instituto de Física del Sur, IFISUR-CONICET, Departamento de Física, Universidad Nacional del Sur, Av. Alem 1253, 8000 Bahía Blanca, Argentina

ABSTRACT

The performance of platinum, gold and copper catalysts with low (0.1 wt%) and high (2–3.8 wt%) metal loadings, supported on ceria with high surface area (240 m^2/g), are contrasted in the hydrogenation of cinnamaldehyde. Two reaction solvents were tested: single-phase near critical CO_2 + isopropanol mixture and supercritical CO_2, both performed at 323 K and 20 MPa. Exceptionally high activities were measured under supercritical CO_2 for low loaded platinum and gold catalysts, while selectivities to cinnamyl alcohol were in the range of 80–90%. The same trends, but in a lower degree, were observed for the corresponding copper sample. The catalytic pattern in near critical condition was between the ones corresponding to supercritical CO_2 and classical gas–liquid, as previously reported for platinum based catalysts. The enhancement of the selectivity can be explained by a combined effect of the supercritical CO_2–substrate interaction and by the adsorption of cinnamaldehyde on sites of the metal–ceria interface. Based on the TPR and XPS characterizations, it was concluded that the rise of the activity would be due to a major concentration of these active sites in the low loaded samples.

© 2015 Elsevier B.V. All rights reserved.

1. Introduction

The employment of supercritical fluids in hydrogenation catalytic processes has been shown to overcome the disadvantages related to conventional gas–liquid processes [1]. In general, gas–liquid catalyzed reactions are diffusion controlled. The use of supercritical fluids reduces this controlling step by eliminating the gas–liquid interface and by increasing the diffusivity of reactants [1]. Therefore, reaction rates are greatly increased and better selectivity can be achieved due to the possibility of uncoupling process variables. For instance, while gas–liquid hydrogenation reactions require high temperatures to increase hydrogen solubility, the temperature of the supercritical process can be modified with no effects in compositions. Supercritical carbon dioxide (scCO_2), is a green alternative because of its particular properties, it is non-flammable, non-toxic, and relatively inert [2]. In addition, unlike organic solvents, the supercritical regime of CO_2 is readily accessible, given its critical temperature of only 304 K.

Selective hydrogenation of α,β-unsaturated aldehydes to unsaturated alcohols is an important reaction in the production of intermediaries used in the pharmaceutical, agrochemical and fragrance industries. The hydrogenation of the olefinic bond is thermodynamically favorable against the hydrogenation of the carbonyl group [3]. Conventional hydrogenation catalysts based on noble metals lead to low yield of cinnamyl alcohol. One strategy for improving the desired selectivity is the employment of no innocent supports [4]. In this sense, ceria has been selected due to its outstanding redox and acid base properties [5]. Ceria strongly modifies the catalytic pattern of Pt, Au and Cu, activating the carbonyl bond and increasing the desired selectivity, which is attributed to the presence of active sites in the metal–ceria interface [3,6,7].

In a previous work, some of us, have studied the selective hydrogenation of cinnamalehyde over Pt(2 wt%)/CeO_2 and Pt(2 wt%)/SiO_2, employing scCO_2 [8]. Higher yield to the unsaturated alcohols than for the case of traditional gas–liquid have been attained. It has been proved that a scCO_2 solvent effect was the responsible for the high catalytic performance [9], while for Pt/CeO_2 additionally a promotional effect of CeO_2 support sites was observed. A peculiar reaction pathway was proposed, with carbonyl adsorption onto the Pt–CeO_2 interface, showing that the nature of the catalyst is of paramount importance for reaching a high catalytic performance under supercritical conditions [8]. From these previous results, it was concluded that the beneficial properties of scCO_2, regarding the high rates for hydrogenation, as well as the effect of

a selective catalyst lead to optimal conditions for performing the hydrogenation of cinnamaldehyde to cinnamyl alcohol.

In the present work, aiming to obtain a selective catalyst for carrying out the hydrogenation of cinnamaldehyde under $scCO_2$, a series of ceria supported catalysts based on Au, Pt and Cu are studied. Samples with metal concentration traditionally employed in the formulation of metal catalysts (2–4 wt%) are utilized. Besides in an attempt to maximize metal dispersion, catalysts with low metal loading (0.1 wt%) are also analyzed. The role of ceria interface sites in the activation of the carbonyl bond is studied in conjunction with the solvent effect of $scCO_2$. The effect of the mass transfer is analyzed comparing the catalytic results corresponding to supercritical CO_2, near supercritical CO_2 + isopropanol and classical isopropanol + H_2 conditions. The catalytic pattern of the ceria supported catalysts is discussed on the basis of the characterization, mainly from TPR, XRD and XPS.

2. Experimental

2.1. Catalysts preparation and characterization

Pt, Cu and Au supported catalysts were prepared. For all the catalysts the support is a high surface ceria, from Rhône Poulenc. This support, from now on, HS–CeO_2 has a specific surface area of 240 m^2/g and a pore volume of 2 cm^3/g.

A platinum catalyst, Pt0.1, was obtained following the incipient wetness method, with aqueous solution of H_2PtCl_6, (Aldrich, 99.8%) with a concentration for obtaining a target Pt concentrations of 0.1 wt%. A copper based sample, Cu0.1, was obtained by means of the wet impregnation method, employing a Cu(AcAc)$_2$ (Aldrich, 99.8%) solution in toluene, with a concentration adjusted in order to obtain copper loading of 0.1 wt%. The solution was contacted with ceria at 333 K in a stirred medium. Following 48 h, the solution was evaporated at 343 K to dryness.

The Au0.1 catalyst was prepared by the direct anionic-exchange method following the procedure of the literature [10]. The support was dried in air at 500 °C and it was put in contact with aqueous solutions of HAuCl$_4$·xH_2O (Alfa Cesar) with concentrations corresponding to target gold loading of 0.1 wt%. The precursor of the gold catalysts were filtered and dried at 373 K.

All the solid precursors of the catalysts were calcined at 773 K, for 4 h under chromatographic air flow (20 cm^3/min).

The metal loading in the samples were determined by atomic absorption spectroscopy, in a Perkin Elmer Analyst 700.

For the sake of comparison, Pt, Cu and Au high loaded samples were also studied. These samples had been previously prepared and characterized [8,11,12]. In the present work, these samples are named as Pt2, Cu3.8 and Au2.

The catalysts were studied by temperature programmed reduction (TPR) employing a home-made apparatus provided with a TCD detector. 0.03–0.2 g of sample was calcined in situ at 773 K for 1 h. The temperature was increased linearly from 293 to 873 K. The reactive mixture was H_2(5%)/Ar, flowing at 20 cm^3/min. The apparatus was calibrated by performing the reduction of known amounts of CuO.

The crystalline characterization of the sample was performed by X-ray Diffraction (XRD). Spectra were obtained in a Philips PW1710 BASED diffractometer equipped with a Cu-Kα radiation source, and a curved detector of graphite operated at 45 Kv y 30 mA with a 0.025°(θ)/s step.

The relative concentration of Ce^{3+} and Ce^{4+} was determined for some of the samples by XPS analysis, which was carried out with a multitechnique specs equipment provided with a dual Mg/Al X-ray source. Spectra were obtained for the For each case, the binding energy (BE) and the area of the corresponding peak were measured.

C 1s, at 284.6 eV, was taken as an internal reference to correct Ce 3d peak position. For Ce, 20 scans were accumulated for increasing the signal-to-noise ratio, whereas for C, 5 scans were accumulated, with 30 eV of pass energy. The peak deconvolutions were performed with a commercial software, taking Scolfield relative sensitive factor 30.50 and 21.12 for 3d 5/2 and 3d 3/2, respectively.

2.2. Catalytic test

2.2.1. Cinnamaldehyde hydrogenation in near critical and supercritical conditions

The experiments were performed in a high pressure reactor as described elsewhere [8]. 0.05–0.1 g of catalyst pre-reduced ex situ at 573 K was wrapped on a filter paper with pore size less than 2 μm and fixed to the magnetic stirrer. Then the catalyst was loaded into the reaction cell along with 0.550 g of cinnamaldehyde. Following purging with CO_2 at 293 K, the cell was filled with liquid CO_2 at 5.8 MPa and 293 K. Afterwards, 6.0 MPa of H_2 at 293 K were loaded. The temperature was raised up to 323 K and a total pressure of 20.6 MPa was reached. The molar fraction of reactants and the solvent were selected following thermodynamic predictions reported in Ref. [14]. Thus the molar fraction of cinnamaldehyde was 0.009, while the corresponding to CO_2 and H_2 were 0.946 and 0.046 respectively. The catalyst/cinnamaldehyde ratio was maintained in the 4–6 range. When isopropanol was used, 1.25 g of alcohol was loaded together with the cinnamaldehyde. The reaction temperature was reached in 10 ± 1.5 min, and at 120 min of reaction time the cell was depressed for stopping the reaction. The reaction mixture was diluted in isopropanol for reaching a concentration of 0.1 M. This procedure ensures low deviations of the chromatography measurements for determining selectivities and conversions. TOF values were calculated in a metal basis, as mole converted per mole of exposed metal (Au, Pt or Cu) atom per second (s^{-1}). Metal particle size of high loaded samples, Au2, Pt2 and Cu4, obtained from the characterization results, were recalculated to metallic dispersion. For further details see Ref. [8,10,11]. For the case of M0.1, the dispersion was considered to be 100%.

The MHV2 model (SRK and Huron–Vidal second-order mixing rule [15]) was followed in order to calculate the phase equilibrium of the H_2/CO_2/cinnamaldehyde and for H_2/CO_2/isopropanol/cinnamaldehyde systems. The critical properties and acentric factors of pure components were obtained from the calculation of Pereda et al. [14]. In previous work [8], the phase envelope (dependence of the pressure vs temperature at constant composition) was reported, showing the equilibrium boundaries for mixtures at x_{cinn} = 0 and at x_{cinn} = 1 for these binary systems (see Fig. 1a in that reference). Based on these results, it was concluded that the experiments using these compositions and performed at 323 K and 20 MPa were conducted within a fluid in single-phase in contact with the solid catalyst, which was verified by naked eye observations during the reactions.

2.2.2. Cinnamaldehyde hydrogenation in liquid phase

The typical procedure was described elsewhere [8,11]. Briefly, 0.150–0.200 g of catalyst previously reduced in H_2 flow at 573 K during 1 h were introduced in the reactor (Parr Instruments, 100 cm^3), avoiding exposure to air. The catalyst was dropped by introducing the glass tube in which reduction took place, into a 0.1 M cinnamaldehyde solution in isopropanol, already introduced into the reactor. The temperature was set at 373 K and the H_2 pressure at 1 MPa. The stirring rate was 800 rpm. When the reaction temperature was reached, the reaction was considered to be started.
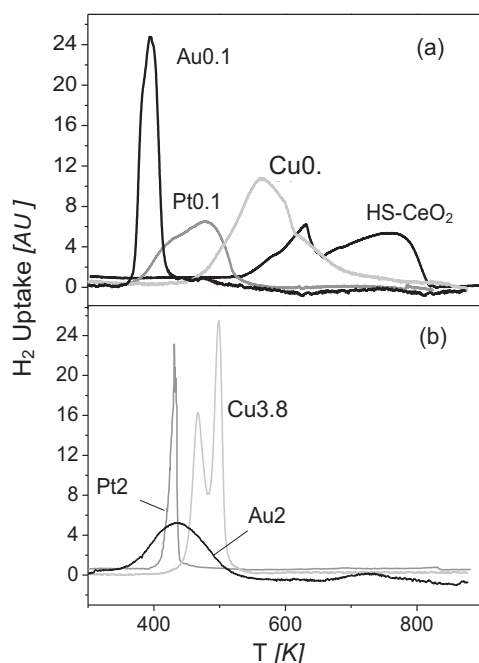
Fig. 1. TPR profiles of HS–CeO$_2$ support and Cu, Pt and Au catalysts. (a) Profiles of 0.1 wt% of metal samples. (b) Profiles of high loaded samples.

Table 1
Redox properties of HAS–CeO$_2$ and Me–CeO$_2$ catalysts, as measured by TPR.

Catalyst	Me (wt%)	T_{max}[b] (K)	H$_2$/Me[b]	Ce^{3+}/Ce^{4+}[c]	Part. size[d] (nm)
HS–CeO$_2$	–	650–780	–	0.29	–
Pt0.1	0.10[a]	490	49.5	0.42	–
Au0.1	0.10[a]	390	51.7	0.43	–
Cu0.1	0.10[a]	590	30.6	0.32	–
Pt2	2.10	410	10.3	0.54	4.2
Au2	1.70	420	22.2	0.34	3.4[e]
Cu4	3.80	460–500	3.3	0.53	9.5

[a] Nominal values.
[b] From TPR characterization.
[c] From XPS characterization.
[d] From XRD characterization.
[e] From TEM characterization.

3. Results

3.1. Catalysts characterization

The metal loading of Pt2, Au2 and Cu4 as measured by AAS are reported in Table 1. For the low loaded samples, the metal concentration was assumed to be the same as the target content, in line with the criterion found in the literature for such metal concentration [13].

3.1.1. TPR

The TPR profiles of the M0.1 catalysts as well as the one of the ceria support are shown in Fig. 1a, while those corresponding to Pt2, Au2 and Cu4 are presented in Fig. 1b.

For the bare ceria, two consumption peaks appeared at temperatures higher than 600 K which would be related with oxygen surface species (peak *circa* 630 K) [6,16] and with the surface reduction of Ce^{4+}–Ce^{3+} (the broad peak in the 650–810 K range).

For all the catalysts, shifts towards lower reduction temperatures were observed, with regards to bare ceria (see Table 1). The enhanced reduction of the support due to the presence of Pt, Cu and Au was previously detected for high loaded samples [8,11]. It is worth to note that in the present work, the shifts were also

achieved for samples (M0.1) with metal loadings at least 10 times lower than the ones corresponding to high loaded catalysts. In the case of M0.1 samples, the H$_2$/Me ratio largely exceeds the unity (see Table 1, fourth column). Thus it should be considered that mainly ceria is responsible for the hydrogen uptake. The role of the metals (Au, Pt and Cu) in Me01, regarding the redox properties of the samples is to weaken Ce–O bond [17]. Large differences in T_{max} of TPR peaks are observed. For example the difference between the maxima of the reduction peaks of Au0.1 and Pt0.1 is approximately 80 °C, while for Cu0.1 the difference is even larger. Thus, although the major responsible for H$_2$ uptake are ceria species, each metal gives a peculiar redox behavior to the corresponding catalyst and Ce–O bond is weakened with more or less intensity according to the nature of the metal: Au, Pt or Cu.

For the case of high loaded samples, the observed peaks are also associated with ceria reduction (see Table 1, fourth column), but the concentration of Au, Pt or Cu is relatively high and these metals play a role *per se* in the redox pattern of the catalysts. Thus the TPR profiles of the high loaded samples are different to the ones corresponding to the low loaded counterparts.

Regarding the quantitative aspects of H$_2$ consumption, in Table 1, fourth column, the specific amount of gas, expressed as mole of H$_2$ per mole of metal is reported. If uniquely the reduction of the metal would be accomplished, following the reaction Me$_x$O$_y$ + yH$_2$ → xMe + yH$_2$O, the H$_2$/Me ratio should be in the 1–1.5 range. However, the reported values of H$_2$/Me largely exceeded the above mentioned theoretical values, showing that support species were engaged in the reduction at relatively low temperature. The exceptionally high hydrogen consumption was previously observed for an Au/CeO$_2$ catalyst [17]. For this catalyst, the reduction peak, at around 367 K, was associated with a high hydrogen consumption (753 μmol g^{-1}), which corresponds to a 30:1 H$_2$/Au molar ratio [17].

The amount of ceria reduced, following the reaction CeO$_2$ + H$_2$ → Ce$_2$O$_3$ + H$_2$O, is reported in the fifth column of Table 1, as Ce^{3+}/Ce^{4+} ratio. This ratio was higher for the catalysts than for the bare support, showing that the reduction of ceria is increased upon the metal incorporation. The support would play an active role in the hydrogenation reaction, due to the enhanced redox properties originated upon the metal introduction. It is surprising that this phenomenon occurs even for extremely low metal concentrations.

The whole of the TPR results shows that the studied catalysts, whatever the metal loading, and whatever the metal considered, present general common trends: ceria reduction is notably enhanced and high specific consumption of hydrogen, at relatively low temperature, are originated upon the introduction of gold, platinum or copper.

3.1.2. XRD and TEM

XRD characterization was carried out for all the catalysts. The diffractogram of CeO$_2$ support is shown in Fig. 2. For the case of the low loaded samples (Cu0.1, Pt0.1 and Au0.1), the diffraction peaks of the corresponding metal species were not detected, due both to the low metal concentration and its high dispersion. In Fig. 2, no other crytalline specie than ceria was observed. On the other hand, for the high loaded copper and platinum catalysts (Cu4 and Pt2 previously published results) the peaks due to CuO and Pt were observed [8,11]. The Scherrer approximation was employed to obtain the particle sizes [19], which are reported in Table 1. For the case of Au2, no diffraction peaks due to the noble metal species were detected. This result had previously been assigned to the fact that gold particles supported on ceria possess sizes lower than 4 nm [20]. A TEM photograph of Au2 is presented in Fig. 3. This picture was taken immediately after reducing the catalyst at 473 K and preserving it in hexane [20]. This procedure was the only method from
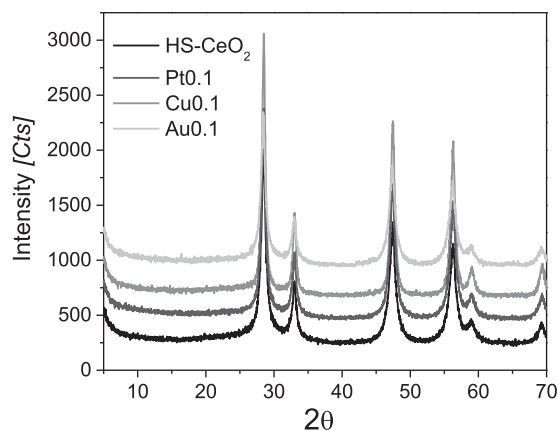
Fig. 2. XRD spectra of HS–CeO$_2$ support and Pt0.1, Cu0.1 and Au0.1 catalysts submitted to the same reduction pretreatment.
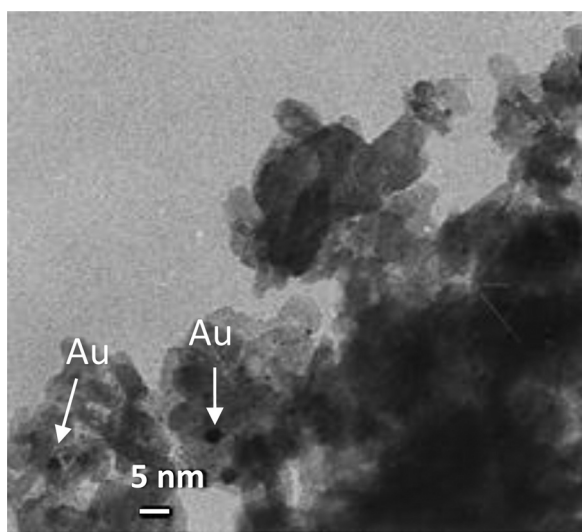

Fig. 3. TEM image of Cu3.8 catalyst after the treatment described in the text.

which some Au particles could be detected in this type of high surface ceria. The statistics of the particles gave an average size of 3 nm, which is in line with XRD results. Since no further information is available for particle size for both gold catalysts, Au0.1 and Au2, and for the low loaded copper and platinum ones, it was not possible to estimate the dispersion of the metal is those samples. Some authors consider that the metal is atomically dispersed on ceria surface up to 0.5 wt% of gold and platinum [13,17,21] and up to 5% for copper [22]. It is known that ceria shows remarkable properties for the dispersion and stabilization of these atomically distributed metals [23,24], which is a reason for selecting ceria as a support in many formulations of catalysts.

3.1.3. XPS

A XPS study was carried out for analyzing the chemical state of the catalysts. The metal loadings are relatively low with regards to the large support specific surface area. For this reason XP peaks of ceria were studied, disregarding the metal ones, for which the signal to noise ratio was excessively low. For Pt2 sample, it was reported that metallic state of platinum is unaltered [8]. However, Si and Flytzani-Stephanopoulos showed that ionic gold (Au$^+$ and Au^{3+}) are the main species in 1 wt% Au on ceria (1 1 0) nanorods catalyst [17], which also exhibited a TPR peak shift, as was commented above.
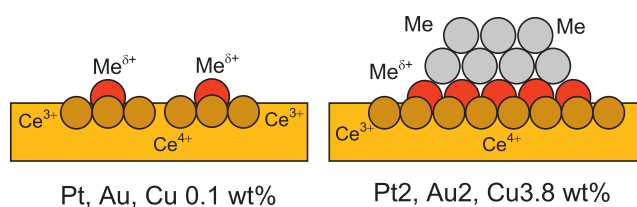
Scheme 1. Representation of the surface species in low and high loaded Au, Pt an Cu catalysts supported on ceria.

The 3d 3/2 and 3d 5/2 peaks of cerium are shown in Fig. 4a–c for the bare support as well as for all the catalysts, submitted to a previous reduction at 673 K. In the 875–925 eV range of BE the v°, v'', u°, and u' peaks, attributed to Ce^{3+} are detected along with the v, v''', v'''', u, u'', and u''' transitions, which are characteristic of Ce^{4+} [25].

From the area of the peaks corresponding to Ce^{3+} and Ce^{4+} respectively, the relative concentration of each species was estimated for the different samples (see Table 1). The Ce^{3+}/Ce^{4+} ratio was higher for the metal catalysts than for the bare support. This result is in agreement with previous studies [26], based on STM and XPS characterization of CeO$_2$ (1 1 1), the authors concluded that the Ce^{4+} concentration in nanostructured ceria thin films decreased after deposition of gold. Considering that the Ce 3d photoelectrons correspond to the region of low kinetic energy, the XPS characterization is related to Ce^{3+} of the very superficial layers (one or two monolayers of the support surrounding the atomically dispersed metal). Once again, it was observed that an extremely low concentration of metal notably modifies the redox properties of the support, in line with the literature [13,17].

In the light of the results corresponding to XPS characterizations, it is concluded that the reduction of cerium species is originated upon Au, Cu or Pt introduction. Such a reduction should be coupled with the oxidation of the metal and the high concentration of Ce^{3+} would be engaged to Me$^{\delta+}$ species. The existence of cationic gold, copper or platinum stabilized by Ce^{3+} on ceria surface was previously detected over CeO$_2$ [13,21,22,24]. For the case of the M0.1 samples, Me$^{\delta+}$ would be the major species, while for the high loaded catalysts the cationic species would coexist with metallic ones. This scenario is depicted in Scheme 1. Certainly the description of the low loaded samples presented in Scheme I was not based on TEM results showing the existence of highly dispersed species (Me$^{\delta+}$). However, this hypothesis fully account for catalytic results, as it will be seen latter, as well as with the behavior reported in the literature [28,29]. Besides, it should be considered that the existence of sub-nanometric metal species being active catalytic sites has been previously postulated for Au and Pt supported on alumina or on ceria [26,28,29]. In all these cases a direct proof of such species from TEM could not be obtained. A more advanced characterization of the catalyst surfaces with atomic-scale resolution techniques and with advanced computational methods would be convenient in order to throw more light in this subject, however, these studies are beyond the scope of the present work.

3.2. Catalytic tests

3.2.1. Hydrogenation of cinnamaldehyde employing scCO$_2$ and near critical CO$_2$ + isopropanol

In Table 2, the conversions achieved after 120 min are reported for all the catalysts tested under supercritical CO$_2$ and near supercritical conditions. The conversion level attained by the bare ceria is 3%. Regarding the results in scCO$_2$, the incorporation of Cu, Pt and Au increased the conversion up to levels as high as 18%. It is astonishing to observe that this fact was accomplished for low amount of
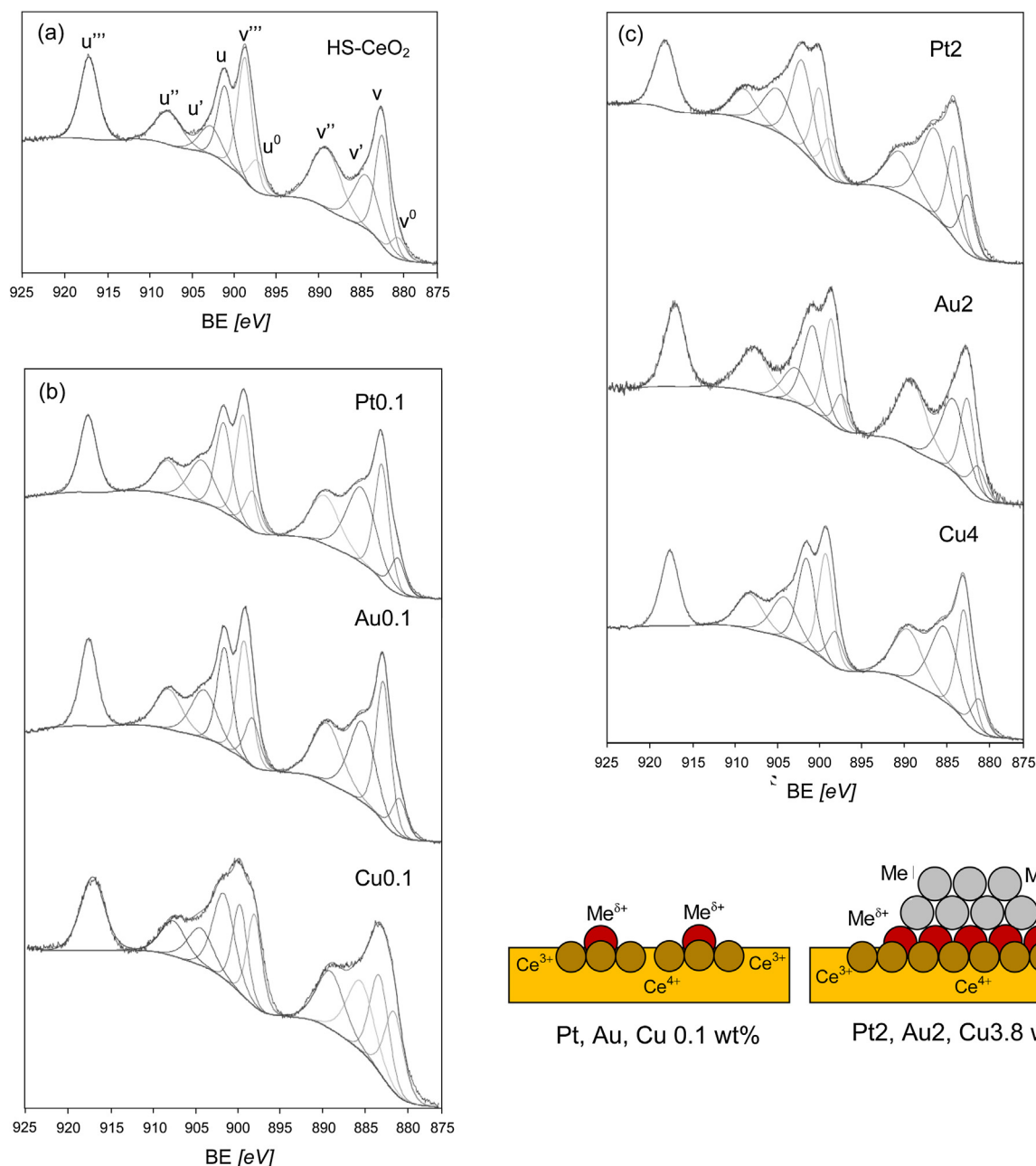
Fig. 4. XPS spectra deconvolution of the ceria and catalysts tested.
(a) HS–CeO$_2$ reduced bare support, (b) Pt0.1, Au0.1 and Cu0.1 catalysts, (c) Pt2, Au2 and Cu3.8 catalysts.

Table 2
Conversion, selectivity to cinnamyl alcohol and TOF for the hydrogenation of cinnamaldehyde in supercritical CO$_2$ and near critical CO$_2$ + isopropanol mixture, 120 min of reaction time.

Catalyst	scCO$_2$			scCO$_2$ + isop		
	X (%)	S (%)	TOF 10^3 (s^{-1})	X (%)	S (%)	TOF 10^3 (s^{-1})
HS–CeO$_2$	3.4	68.5	–	3.1	51.4	–
Pt0.1	10.3	90.6	148	6.1	65.6	86.2
Au0.1	6.7	75.4	97	4.3	59.8	62.4
Cu0.1	5.5	73.1	26	3.4	25.7	15.4
Pt2	10.2	80.3	9	8.9	83.5	7.2
Au2	5.4	55.5	8	4.3	67.3	6.2
Cu4	18.0	8.0	6	14.0	28.0	4.3

metals. For Pt and Au practically the same conversions are obtained for M0.1 than for the counterpart catalysts with a much higher concentration of metals. This fact leads to TOF values one order of magnitude higher for M0.1 than for the more loaded samples (see Table 2). In the same line, previous report of Yi et al. reported one order of magnitude of difference in methanol steam reforming activity in low loaded Au–CeO$_2$ catalysts, when Au–Ce interaction is present [28]. Undoubtedly, a strong synergic effect is developed between the metals and the ceria support for the M0.1 samples.

It is important to recall that it is not possible to measure the particle size for the M0.1 samples, thus the corresponding metallic dispersions were not available for calculating TOF values. As mentioned above, ceria oxide promotes dispersion of platinum [30], gold [13,17] and copper [31]. In line with this, 100% dispersion is assumed for Cu0.1, Pt0.1 and Au0.1 and the corresponding TOF were calculated based on such high dispersion (see Table 2). If the metals would not be atomically dispersed on ceria, the dispersion would be lower than 100%. In this case even higher TOF than the ones reported in Table 2 would be obtained.

It should be considered that probably the actual active site is a complex combination of metal and support sites. Since a complete description of such a site is not available, TOF values based on metal and cerium atoms are not available. Anyway, TOF values calculated on Au, Pt or Cu basis is a general way to compare the different catalysts and allow to establish general comparisons between low and high loaded Au, Pt or Cu catalysts.

In view of the whole characterization results and the catalytic properties developed under $scCO_2$, the model of the catalysts presented in Scheme 1, matches these results. It is postulated that Me–Ce^{3+} species are the key sites responsible for the hydrogenation of cinnamaldehyde. For the case of M0.1, the fraction of Me–Ce^{3+} is high, thus this leads to exceptionally high TOF values and high selectivities For the case of high loaded samples, the fraction of Me–Ce^{3+} is low giving rise to standard TOF values.

Regarding the selectivity, the low loaded samples are more selective than high loaded ones, reaching 90% for Pt0.1. However, some differences arise when the three M0.1 catalysts are compared form the point of view of the catalytic performance. Pt–Ce^{3+} sites are the most active and selective sites, while Cu–Ce^{3+} shows the lowest activity and selectivity.

Previously, a promotional solvent effect of $scCO_2$ on the selective hydrogenation of α,β-insaturated aldehydes was concluded [9]. However, for the ceria supported catalysts studied in the present work, the $scCO_2$ solvent effect becomes eclipsed by the high specific activity of Me–Ce^{3+} sites [8]. Still another possible effect should be considered: the nature of metal particles could be modified by electron transfer to carbon dioxide, as suggested by Arai et al. [32].

The reaction performed in single-phase with near critical isopropanol + CO_2 mixture, showed similar trends than the ones observed under $scCO_2$: higher activity and selectivity for low loaded samples than for high loaded ones. However, minor differences between the M0.1 samples and the ones with a higher concentration of metals were observed. The supercritical solvent highlights the catalytic differences between low and high loaded samples, due to the fact that the chemical aspects of the catalytic reaction are practically not influenced by any other phenomena. The inclusion of isopropanol shifts the supercritical zone to higher temperatures, rising mass transfer limitations and diluting the $scCO_2$–substrate and/or $scCO_2$ interactions [8]. The mass transfer properties of the solvents should differ considerably since $scCO_2$ and near critical CO_2 + isopropanol viscosities are 0.108 and 0.036 cP respectively according to the corresponding states model suggested by Pedersen and Fredenslund [33].

When comparisons of the catalytic properties are performed between the three metals, disregarding the metal loadings, differences arise, showing that each Me–Ce^{3+} sites possess particular features. The order of activity is, for both series, low and high loaded ones, Pt > Au > Cu. It is worth to note that this order is the same as the one previously measured for samples tested under classical gas–liquid conditions [6,10,11]. in which case Pt based catalyst were more active than gold and copper ones. The same conclusion is reached for selectivity, since the same order of increasing selectivity was measured for $scCO_2$ (see Table 2) than under classical liquid phase conditions.

In previous works it was reported that the supercritical solvent activates C=O, giving rise to an enhanced selectivity of Pt(1–2 wt%)/SiO_2 catalysts [8,34]. However it was concluded that when supporting 2 wt% Pt on HS–CeO_2 the beneficial properties of $scCO_2$ were in some way diminished. In that work we proposed that surface chemistry prevails over the $scCO_2$–substrate interaction [8]. From the present results, it is concluded that copper, platinum or gold species, highly interacting with the HS–CeO_2 support are highly selective. Specifically for the case of the M0.1 samples, the selectivity is mainly ruled by Me–Ce^{3+} sites, while the $scCO_2$ solvent effect plays a secondary role, in accordance with our previous

suggestion. In this way, it is concluded that the chemical nature of the catalyst is extremely important when reactions are carried out in supercritical conditions.

Finally it is worth to note that the hydrogenation of cinnaldehyde was also performed under classical gas–liquid conditions using the Cu0.1, Pt0.1 and Au0.1 catalysts. Low value of conversions were reached (<1%) and selectivity was generally conducted to saturated aldehyde, thus low yields to cinnamyl alcohol were achieved. The enhanced yield reached under supercritical conditions for the low loaded samples was not achieved for classical conditions. Hydrogen concentration in liquid phase (0.00815 M) and mass transfer limitations should be responsible for this performance, since the viscosity of isopropanol at 373 K and 0.4 MPa, calculated by the same model mentioned above, results in 0.29 cP.

Summing up, highly active and selective Me–Ce^{3+} sites are developed when low amounts of platinum, gold and copper are supported on ceria.

4. Conclusions

Highly selective and active sites are obtained over low loaded (0.1 wt%) platinum, gold and, in a lesser extent, copper catalysts supported on high surface area ceria. This is due to the formation of highly interacting metal-support sites, Me–Ce^{3+}.

Under supercritical conditions the synergic metal-support effect leads to exceptionally active and selective sites for the hydrogenation of cinnamaldehyde, thus high yields are obtained over ceria catalysts with metal loading of 0.1 wt%.

The nature of the catalyst strongly influence on the catalytic pattern developed under $scCO_2$ solvent.

Besides, this work is linked with the developing of catalysts with low precious metal content, in the context of the scarcity of natural resources and the increasing price of precious metals [35,36,37]. And it is concluded that it is possible to obtain highly active a selective catalysts for hydrogenation reactions employing catalysts with very low loading of metals.

Acknowledgements

References

[1] E. Weidner, C. Brake, D. Richter, in: G. Bruner (Ed.), Supercritical Fluids as Solvents and Reaction Media, Elsevier B.V., Hamburg, 2004, pp. 269–295.
[2] E. Beckman, J. Supercrit. Fluids 28 (2004) 121–191.
[3] M. Arai, H. Takahashi, M. Shirai, Y. Nishiyama, T. Ebina, Appl. Catal. A: Gen. 176 (1999) 229–237.
[4] L. Vivier, D. Duprez, ChemSusChem 3 (2010) 654–678.
[5] N. Ichikawa, S. Sato, R. Takahashi, T. Sodesawa, J. Mol. Catal. A: Chem. 231 (2005) 181–189.
[6] B. Campo, S. Ivanova, C. Gigola, C. Petit, M. Volpe, Catal. Today 133–135 (2008) 661–666.
[7] J. Lenz, B. Campo, M. Alvarez, M. Volpe, J. Catal. 267 (2009) 50–56.
[8] C.M. Piqueras, V.S. Gutierrez, D.A. Vega, M.A. Volpe, Appl. Catal. A: Gen. 467 (2013) 253–260.
[9] J. Wang, M. Wang, J. Hao, S. Fujita, M. Arai, Z. Wu, F. Zhao, J. Supercrit. Fluids 54 (2010) 9–15.
[10] V. Gutierrez, M. Alvarez, M. Volpe, Appl. Catal. A: Gen. 437–438 (2012) 72–78.
[11] V. Gutierrez, M. Alvarez, M. Volpe, Appl. Catal. A: Gen. 413–414 (2012) 358–365.
[12] B. Campo, G. Santori, C. Petit, M. Volpe, Appl. Catal. A: Gen. 359 (2009) 79–83.
[13] N. Yi, H. Saltsburg, M. Flytzani-Stephanopoulos, ChemSusChem 6 (2013) 816–819.
[14] S. Pereda, S. Bottini, E. Brignole, Appl. Catal. A: Gen. 281 (2005) 129–137.
[15] S. Dahl, M.L. Michelsen, AIChE J. 36 (1990) 1829–1836.
[16] S. Lai, Y. Qiu, S. Wang, J. Catal. 237 (2006) 303–313.

[17] R. Si, M. Flytzani-Stephanopoulos, Angew. Chem. Int. Ed. 47 (2008) 2884–2887.
[19] J. Scholten, A. Pijpers, M. Hustings, Catal. Rev. Sci. Eng. 27 (1985) 151–206.
[20] B. Campo, M. Volpe, S. Ivanova, R. Touroude, J. Catal. 242 (2006) 162–171.
[21] Q. Fu, H. Saltsburg, M. Flyzani-Stephanopoulos, Science 301 (2003) 935–938.
[22] P. Bera, S. Aruna, K. Patil, M. Hegde, J. Catal 186 (1999) 36–44.
[23] M. Flytzani-Stephanopoulos, B.C. Gates, Annu. Rev. Chem. Biomol. Eng. 3 (2012) 545–574.
[24] Q. Fu, W. Deng, H. Saltsburg, M. Flytzani-Stephanopoulos, Appl. Catal. B: Environ. 56 (2005) 57–68.
[25] F. Larachi, J. Pierre, A. Adnot, A. Bernis, Appl. Surf. Sci. 195 (2002) 236–250.
[26] M. Baron, O. Bondarchuk, D. Stacchiola, S. Shaikhutdinov, H.J. Freund, J. Phys. Chem. C 113 (2009) 6042–6049.
[28] N. Yi, R. Si, H. Saltsburg, M. Flytzani-Stephanopoulos, Energy Environ. Sci. 3 (2010) 831–837.

[29] N. Yi, R. Si, H. Saltsburg, M. Flytzani-Stephanopoulos, Appl. Catal. B: Environ. 95 (2010) 87–92.
[30] M. Hatanaka, N. Takahashia, T. Tanabe, Y. Nagai, K. Dohmae, Y. Aoki, T. Yoshida, H. Shinjoh, Appl. Catal. B: Environ. 99 (2010) 336–342.
[31] Y. Hung, L. Dong, M. Shen, D. Liu, J. Wang, W. Ding, Y. Chen, Appl. Catal. B: Environ. 31 (2001) 61–69.
[32] M. Arai, Y. Nishiyama, Y. Ikushima, J. Supercrit. Fluids 13 (1998) 149–153.
[33] K.S. Pedersen, A. Fredenslund, Chem. Eng. Sci. 41 (1987) 182–186.
[34] B.M. Bhanage, Y. Ikushima, M. Shirai, M. Arai, Catal. Lett. 62 (1999) 175–177.
[36] D.W. Flaherty, S.P. Berglund, C.B. Mullins, J. Catal. 269 (2010) 33–43.
[37] M. Hatanaka, N. Takahashi, N. Takahashi, T. Tanabe, Y. Nagai, A. Suda, H. Shinjoh, J. Catal. 266 (2009) 182–190.